



ISSN: 2723-9535

Available online at www.HighTechJournal.org

HighTech and Innovation Journal

Vol. 3, No. 1, March, 2022



Evaluation and Optimization of the Aerodynamic Noise Reduction of Vehicle Side View Mirrors: Experimental and Numerical Study

Mohammad Gohari ^{1*} , Rasoul Norozi ¹, Abolfazl Hajizadeh Aghdam ¹

¹ Department of Mechanical Engineering, Arak University of Technology, Arak, Iran.

Received 17 November 2021; Revised 09 January 2022; Accepted 17 January 2022; Published 01 March 2022

Abstract

Automobile passengers are usually sensitive to the noises generated by the engine and vehicle body. One of the noise sources is the generated turbulent flow around the Vehicle Side View Mirror (VSVM) and around the A-pillar, producing fluctuating pressure. Unwanted noise is a result of fluctuating pressure around the car's body. Modification of the geometry of the vehicle body may affect the generated noise by turbulent flow. In this paper, the original side view mirror of a small sedan car named Tiba was aimed at geometry modification to decrease airborne noise. The mirror was assessed by CFD simulation and an outdoor test. Road tests were applied at three forward speeds (80, 100, and 120 km/h) to measure the sound level generated by the vehicle's side mirrors. Then, the geometry of VSVM was modified to diminish the sound pressure level of that based on decreasing turbulent flow and fluctuating pressure around the side mirror. Finally, the achieved geometry was evaluated using road tests, which showed a noise reduction of 8 to 12%. Road tests were done for the modified side car mirror. It shows that a modified mirror can reduce the sound level of airborne noise. By using this suggested modified side view mirror, the risk of annoying noise may be diminished and passenger comfortability can be increased through driving.

Keywords: Aerodynamic Noise; Vehicle Side View Mirror Noise; CFD; Optimization.

1. Introduction

Aerodynamic noise is one of the dominant noise sources that occurs in high-speed vehicles. The main sources of this type of disturbing noise are A-pillars, side view mirrors, tire rings, and fans. Aeroacoustic characteristics have negative effects on vehicle customers' feelings. The frontier engineering modeling that was presented to describe this phenomenon is the Lighthill Equations [1, 2]. Many studies were carried out to reduce aeroacoustic noises and increase driver comfort and riding quality. Automobile side view mirrors are used to develop driver vision, but they generate aeroacoustic noise due to their geometric properties. In some research using wind tunnels, the pressure around a mirror was studied [3, 4]. In addition, hot wires were employed to investigate turbulent fluid distributions that are created around mirrors [5]. Those studies identified critical points on the mirror surface that have a significant impact on noise generation. Furthermore, the effects of wind direction on generated noise were studied [6]. Moreover, sound levels were measured by various instruments to find the area that creates sound and noise in a vehicle's body [1]. The results of these investigations show that a major portion of the external noise comes from turbulent fluid produced by mirrors.

* Corresponding author: moh-gohari@arakut.ac.ir; moh.gohari@gmail.com

 <http://dx.doi.org/10.28991/HIJ-2022-03-01-08>

➤ This is an open access article under the CC-BY license (<https://creativecommons.org/licenses/by/4.0/>).

© Authors retain all copyrights.

Researchers used Computational Fluid Dynamics (CFD) to study and optimize mirror geometry optimization for low aerodynamic noise [7-9]. The optimized car side mirror by CFD simulation showed that the sound level decreased in outdoor experiments [10]. In theory, the acoustic energy density and intensity at a field point Y are stated based on the acoustic velocity and the acoustic pressure as [11]:

$$\langle e_Y \rangle = \frac{1}{4} [\rho \widehat{v}_Y \cdot \widehat{v}_Y^* + \frac{1}{\rho c^2} \widehat{p}_Y \cdot \widehat{p}_Y^*] \tag{1}$$

$$\langle I_Y \rangle = \frac{1}{2} R(\widehat{p}_Y \cdot \widehat{v}_Y^*) \tag{2}$$

Where ρ is the density of the acoustic medium, subscript “Y” shows a quantity associated with a field point Y, c is the velocity of the sound in the medium, \widehat{v} and \widehat{p} are the acoustic speed and the acoustic pressure, respectively. Thus, the generated sound intensity depends on the pressure and velocity of the fluid around an object. Based on the stated theory, some investigations were applied to vehicle side mirrors. The effect of the presence of a side mirror was studied by numerical modelling. It shows that the A-pillar is the main source of noise in the absence of a mirror, while in the presence of a vehicle side mirror, the mirror is the main source of noise [12]. In addition to the airborne noise generated by the car's side mirror, vehicle windows vibrate due to the fluctuating pressure of the mirror. These vibrations cause uncomfortable interior noise for the passengers [13]. In another study, a clay model of a vehicle was tested in the wind tunnel. The results show that the main source of transmitted interior noise is related to the mirror [14]. The Lighthill theory was used to make a numerical model to investigate the effect of the mirror and A-pillar on noise generation. The modelling research shows that the noise from the A-pillar is higher than the noise from the side view mirror in the whole frequency range [15]. Furthermore, via a generic model and experimental test in a wind tunnel, noise reduction in the vehicle body was carried out. The rear-view mirror was attached to the vehicle body by a slotted solid base. The experimental outcome demonstrates that higher noise decreases can be attained with the increase of airflow rate through the slot. In addition, the results show that the negative pressure zone in the side view mirror wake area declines and the vortex center moves upward away from the vehicle wall surface, decreasing the aerodynamic noise from the plate surface [16]. Moreover, the interaction of a simplified car model and airflow was studied to understand acoustic noise sources by finite element modelling. As with other investigations, this modeling emphasized that the side view mirrors produce interior noise in the vehicle [17].

Via the mentioned achievements of studies, geometry modification of side mirrors and noise reduction can be attained. By geometry, modification can change these parameters, and consequently the sound pressure can be diminished. Based on a survey carried out among Tiba drivers (a small sedan manufactured by SAIPA Co.), they stated that the transmitted noise to the passengers is not neglect able. Referring to the specified theory of airborne noise and the complaints of drivers, the current study is focused on the side view mirror noise reduction of the Tiba, a small sedan vehicle manufactured by SAIPA, Iran. This effort in noise reduction is described in the following.

2. Research Methodology

In the first step, the current side view mirror of Tiba was tested by outdoor experiments at three forward speeds (80, 100, and 120 km/h). The sound level was recorded via sound data gathering (DAQ) connected to the microphone. Next, the current mirror was modeled and simulated in ANSYS/Fluent Software. The results of the simulation were compared to the outdoor test. Finally, the optimized geometry of the mirror was acquired by CFD and it was tested by outdoor experiments. In the following, the procedure for these steps is described in detail.

2.1. CFD Simulation of Current Model

The sizes and angles of Tiba mirrors were measured accurately, and a model was drawn in Solidworks Software, which is shown in Figure 1. The 3D model was imported into ANSYS FLUENT for analysis. A rectangle space was generated as a duct, which included a mirror. The 3D model was meshed, which is exhibited in Figure 2. The parameters of Broadband solution are stated in Table 1.

Table 1. Simulation parameters

Velocity inlet	33.33 , 27.77 , 22.22 (m/s)
Pressure outlet	0 (pa)
Fluid	Air
Analyze model	Broadband [k, ε]
Flow	Turbulence
Mesh	Tetrahedron
Number of Elements	1450953
Element size 1-Layer	0.01 (m)
Element size 2-Layers	0.1 (m)

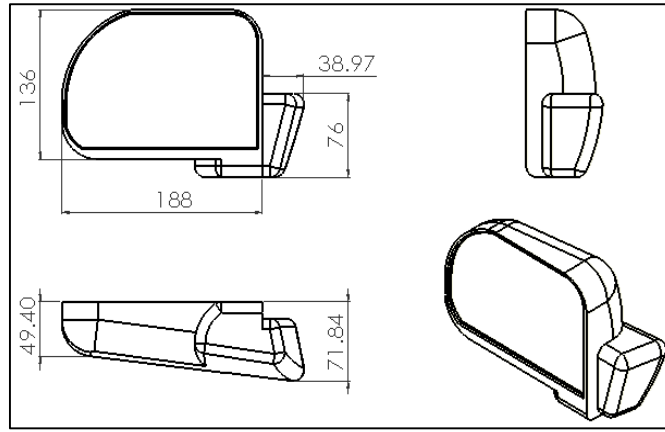


Figure 1. Tiba Mirror modeled in Solidworks Software (unit: milimeter)

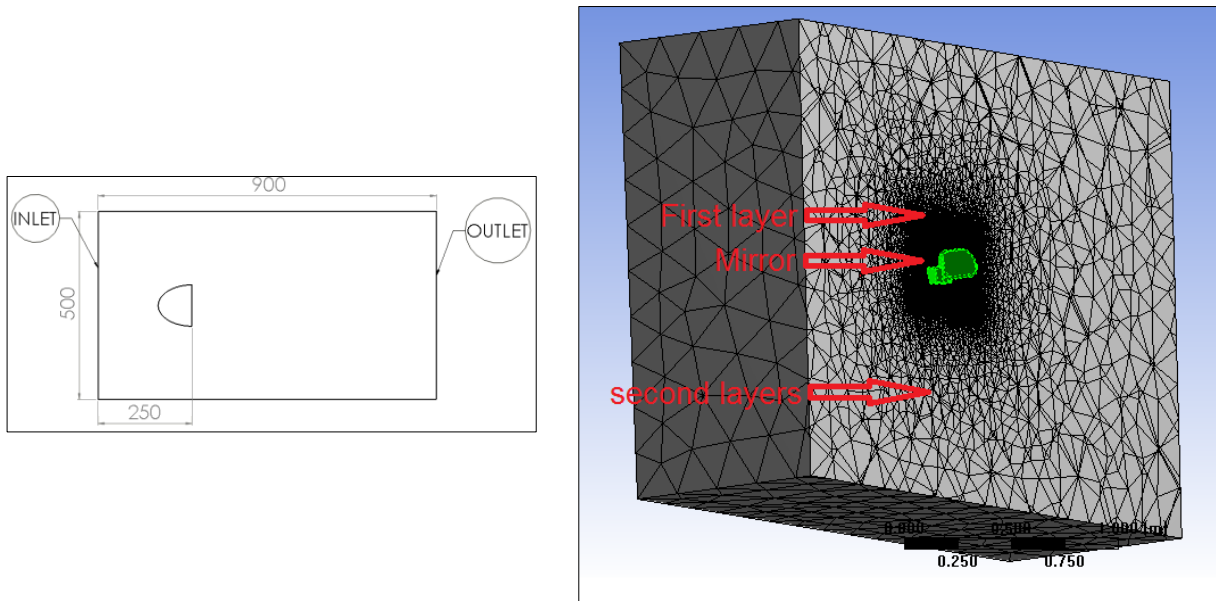
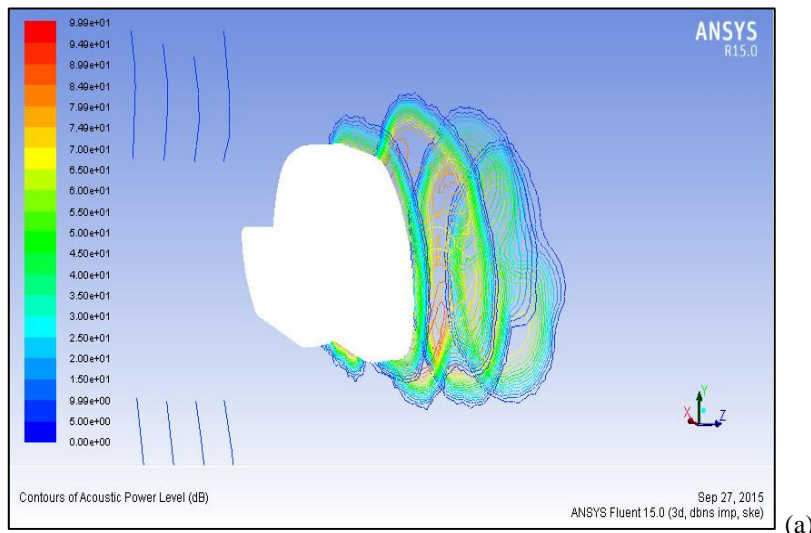


Figure 2. Two size meshes which were used, and size of corridor (unit: milimeter)

3. Results and Discussion

The sound levels were reached at three forward speeds. At 120 km/h, the maximum sound level was around 99.9 db. In Figure 3, the sound levels in the X and Z directions are revealed. Similarly, sound levels were obtained at 91 and 87 db at 100 and 80 km/h, respectively.



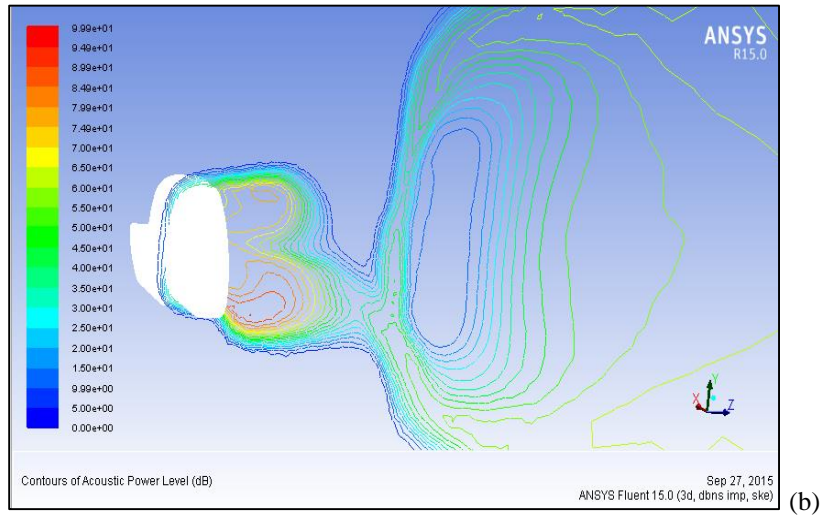
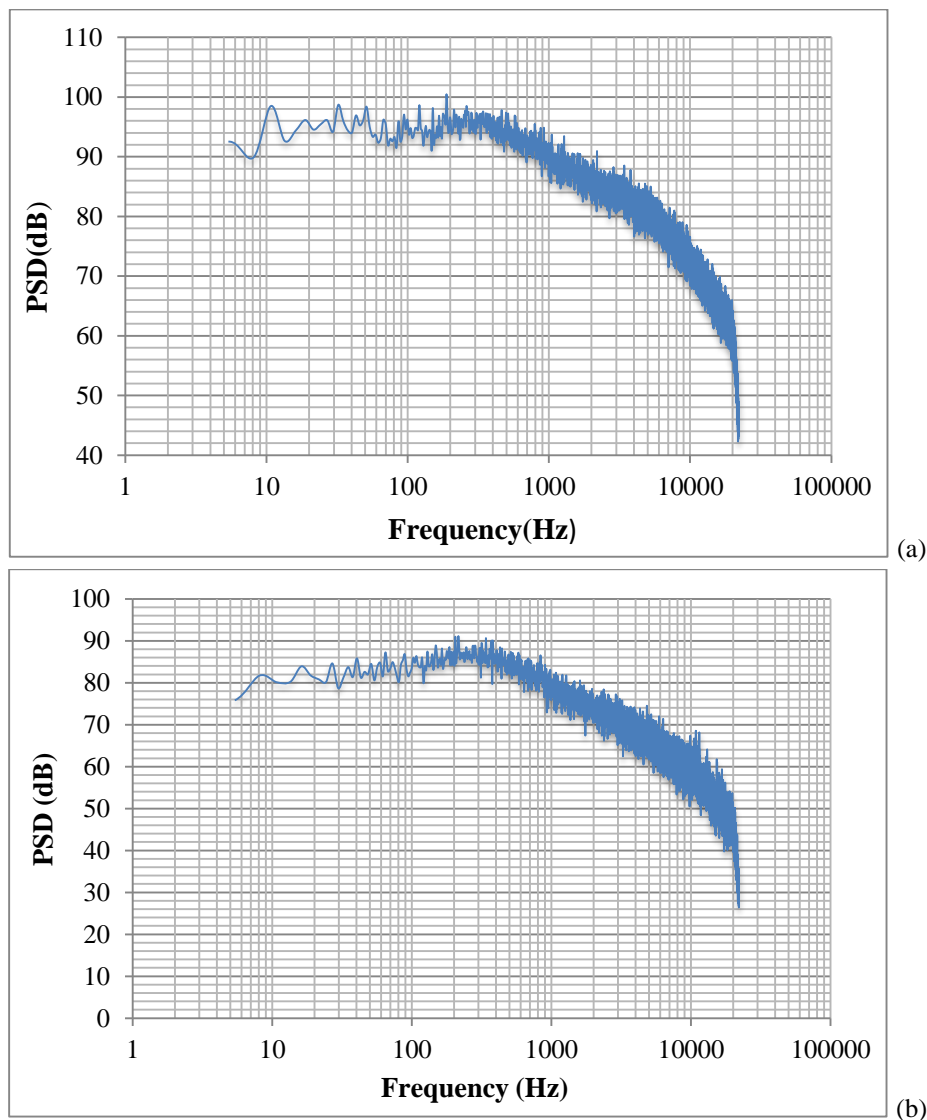


Figure 3. (a) Sound level in X-direction, (b) sound level in Z-direction (120 km/h)

3.1. Outdoor Test of Current Mirror

The pressure sound levels of the side view mirror were measured by an installed microphone at three forward speeds. The results of the outdoor tests at three forward speeds are presented in Figure 4. As can be found, there is a closeness between CFD simulation and outdoor test sound level measurements. The maximum sound pressure levels were recorded at 86, 94, and 101 db at 80, 100, and 120 km/h, respectively.



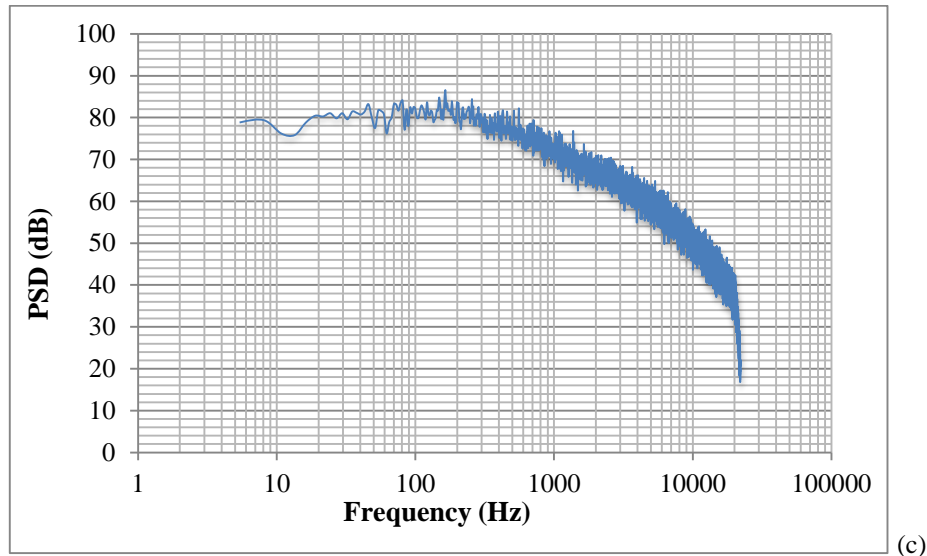


Figure 4. The maximum sound pressure level measured in outdoor test: (a) 120 km/h, (b) 100 km/h, and (c) 80 km/h

3.2. Geometry Optimization of Mirror

To decrease the generated sound level of the current side view mirror, first a 2D simulation was done to avoid a time-consuming problem solving process. Through this simulation, the proper cross area of the mirror in 2D space was reached. Next, this achieved 2D cross area was converted to 3D space by extrusion.

2D Cross Area Optimization

To obtain best cross area of mirror, a half elliptical shape was considered which has two variable diameters: C and D [11, 18]. This cross area is illustrated in Figure 5.

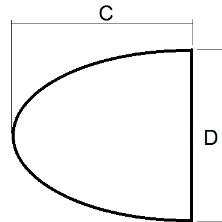


Figure 5. Cross area of mirror which is considered to optimise

In the 2D CFD simulation, the vertical diameter (D) was kept constant at 136 mm and the horizontal diameter (C) was changed from 40 to 145 mm. For each iteration, the CFD solution was done for three forward speeds: 80, 100, and 120 km/h. Subsequently, C was kept constant at 90 mm and D was changed. With this scenario, 110 solutions were executed. The minimum sound level was gained with C=90 and D=110 mm. Figure 6 reveals sound pressure levels by C and D variations. The selected cross area generated 94 db at a 120 km/h speed. Also, sound pressure levels were attained at 90 and 85 db at 100 and 80 km/h, respectively.

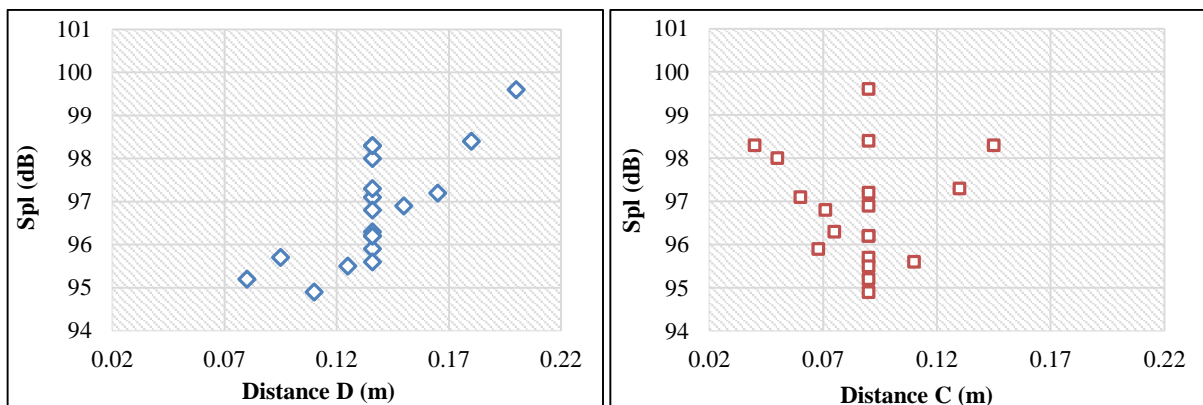


Figure 6. variation in sound level by variation of C and D

The sound pressure level contours and kinetic energy in 2D simulation are shown in Figure 7.

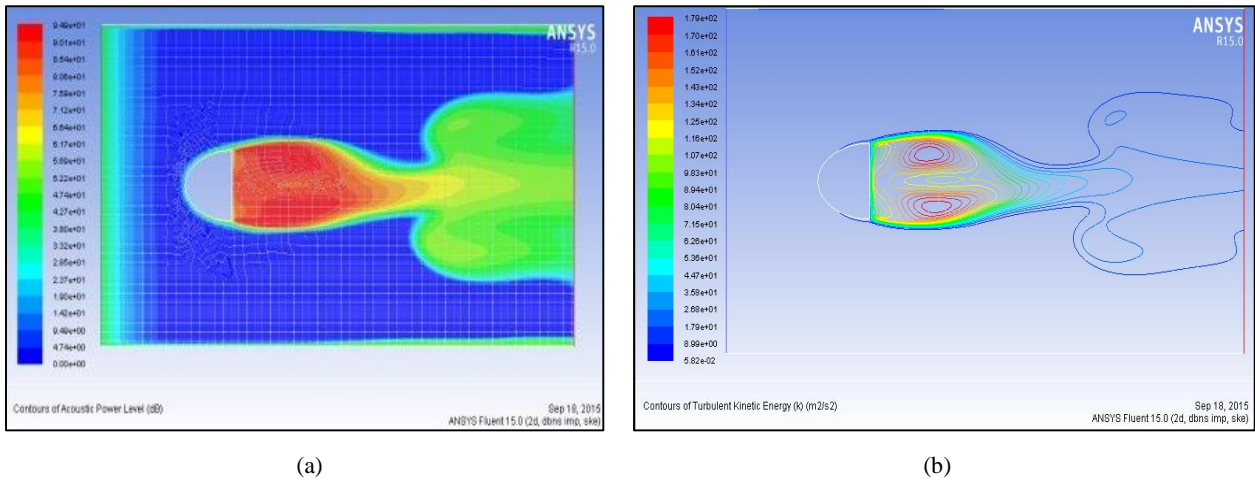


Figure 7. (a) Sound pressure level contours, (b) Kinetic Energy

3D CFD Simulation for Optimized Cross Area

The attained 2D cross area was extruded into a 3D model, and CFD simulation was performed to acquire the sound pressure level of that. The results are presented in Figures 8 to 11 at various forward speeds. The sound pressure levels were achieved at 89, 85, and 80 db at 120, 100, and 80 km/h, respectively.

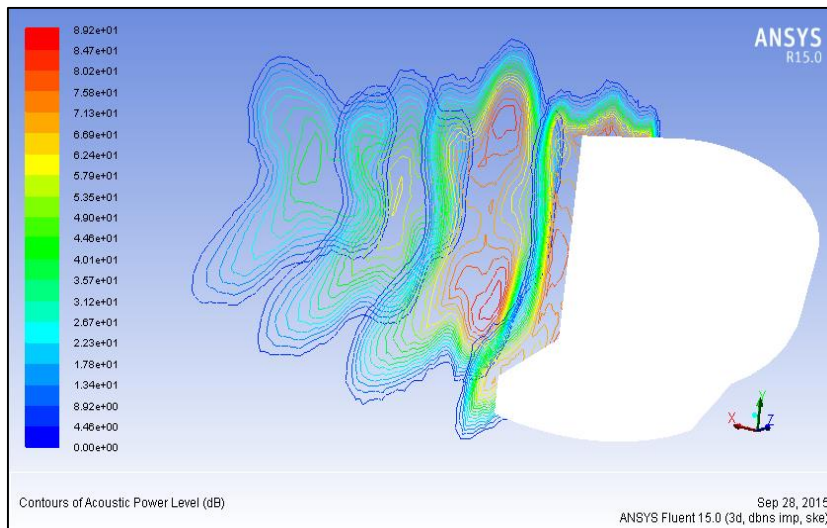


Figure 8. Sound pressure level in Z-direction (120 km/h)

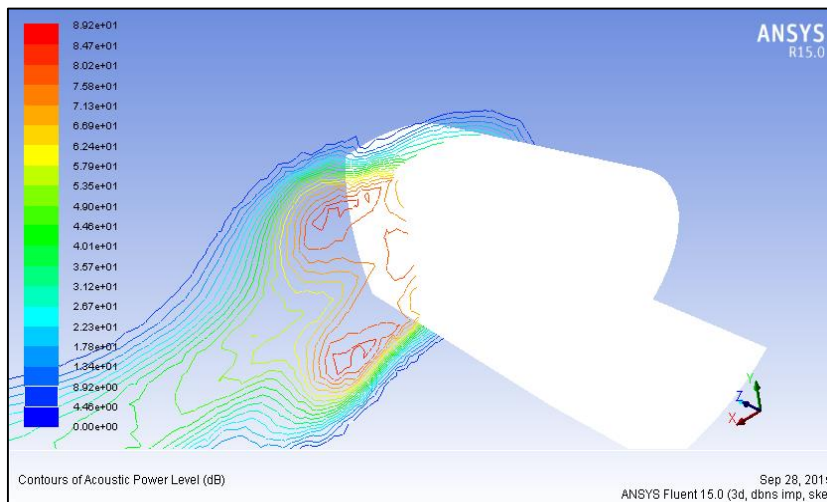


Figure 9. Sound pressure level in X-direction (120 km/h)

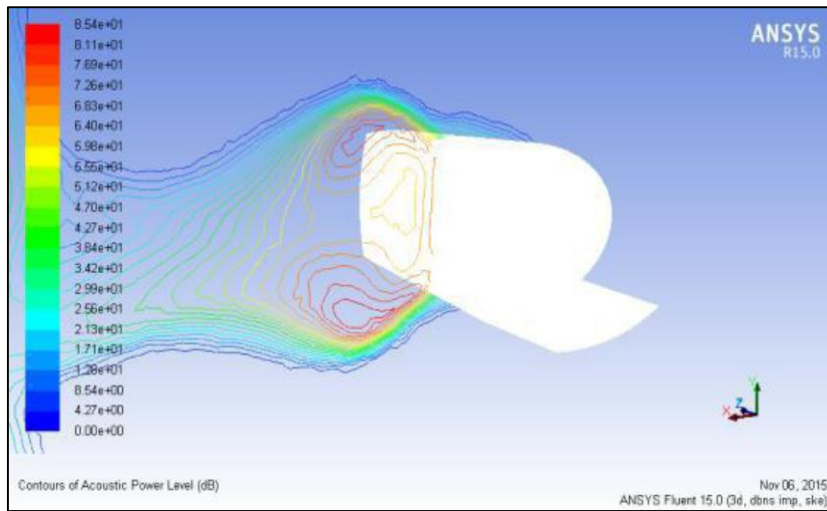


Figure 10. Sound pressure level in X-direction (100 km/h)

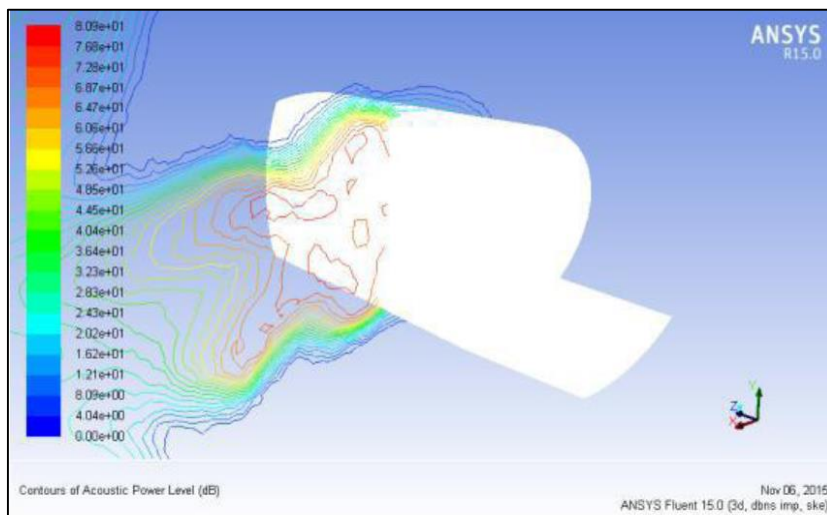


Figure 11. Sound pressure level in X-direction (80 km/h)

Furthermore, stream line velocity and pressure contours were computed by ANSYS FLUENT Software for both the current Tiba mirror and the modified mirror. Figure 12 shows the stream line velocity of the Tiba mirror, and Figure 13 illustrates the velocity contours of the modified mirror at 120 km/h forward speed. As can be seen in these pictures, the turbulent zone in the back of the modified mirror is smaller than the current mirror due to the reduced area of fluctuating pressure. As with other efforts, the maximum velocity zone is located on the edge [3, 19-24]. The maximum speed of the modified was 44.3 m/s, while this value was 60 m/s for the current Tiba mirror.

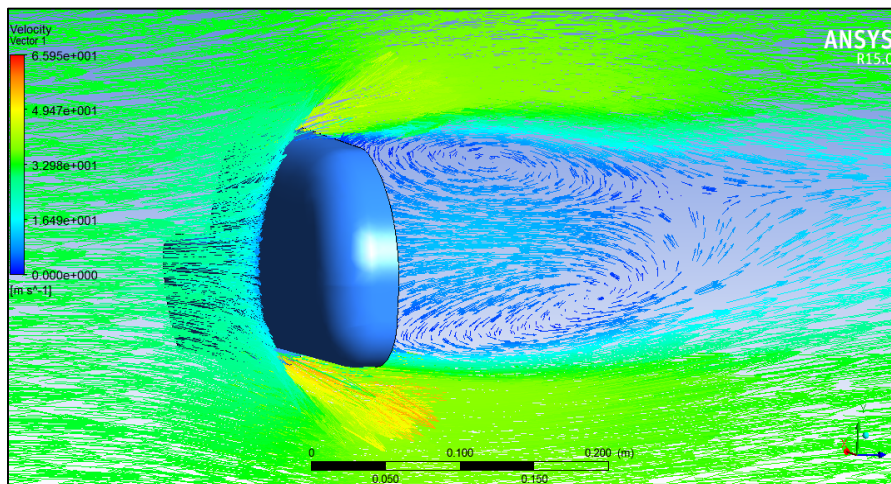


Figure 12. Velocity contours of current Tiba mirror (120 km/h)

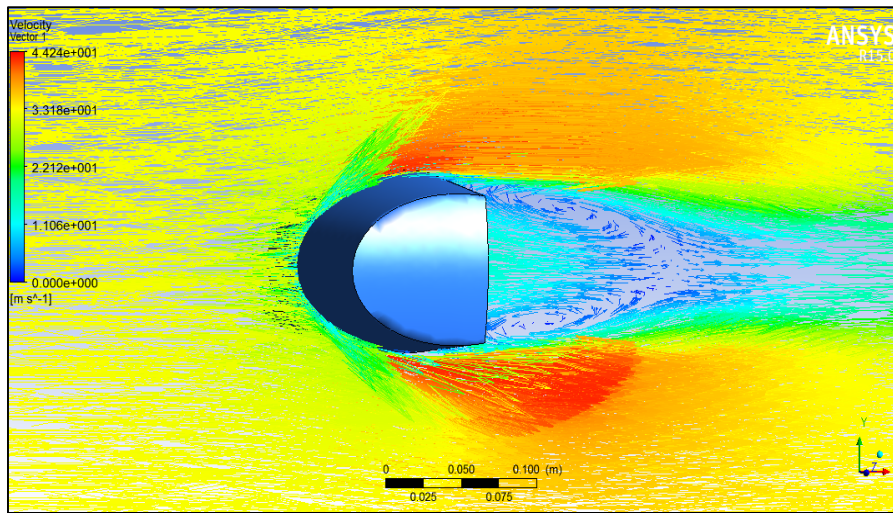


Figure 13. Velocity contours of modified mirror (120 km/h)

In addition to velocity and pressure contours, the current mirror and modified mirror are exhibited in Figure 14. As can be observed, the high pressure zone in the current mirror is larger than in the proposed mirror. The maximum pressure for the proposed mirror is 689 Pa, though this value is attained at 704 Pa with the current mirror. It means that the fluctuating pressure zone is limited by modified geometry, and it reduces turbulent air flow behind the side mirror. High velocity zones and low pressure zones provide a better understanding of places that may generate aerodynamic noise [25-27].

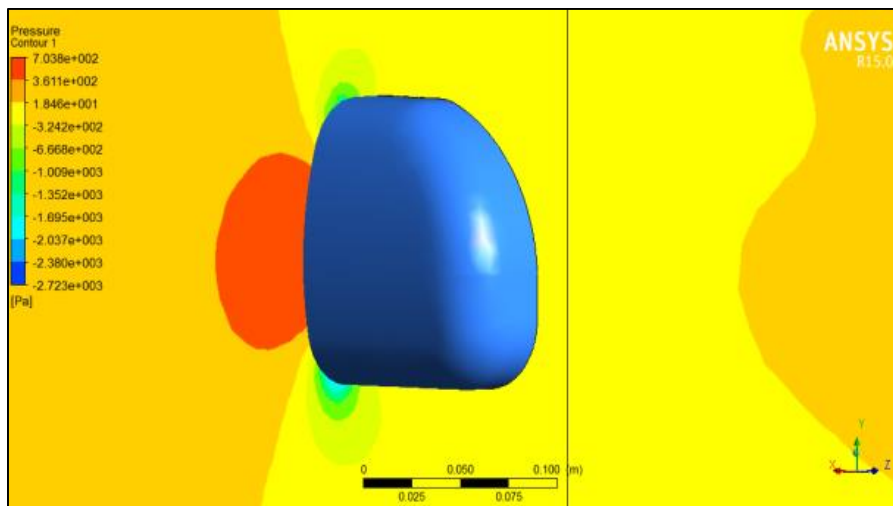


Figure 14. Pressure contours in current mirror (120 km/h)

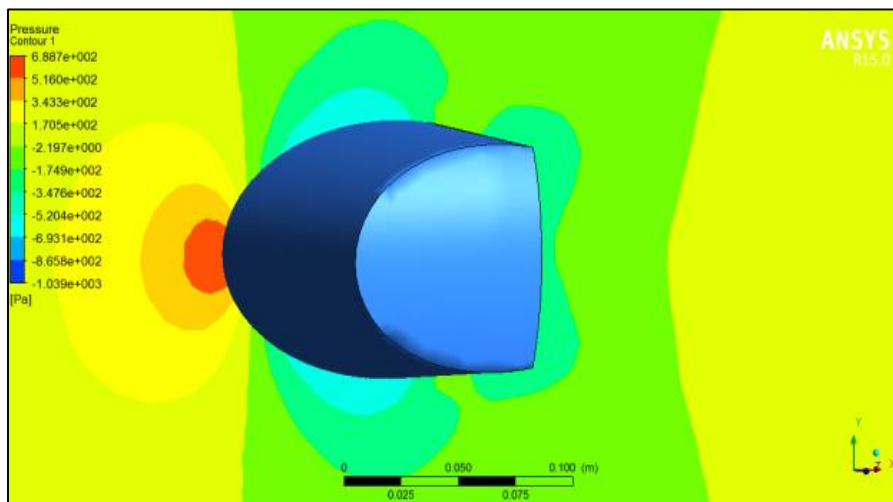


Figure 15. Pressure contours in proposed mirror (120 km/h)

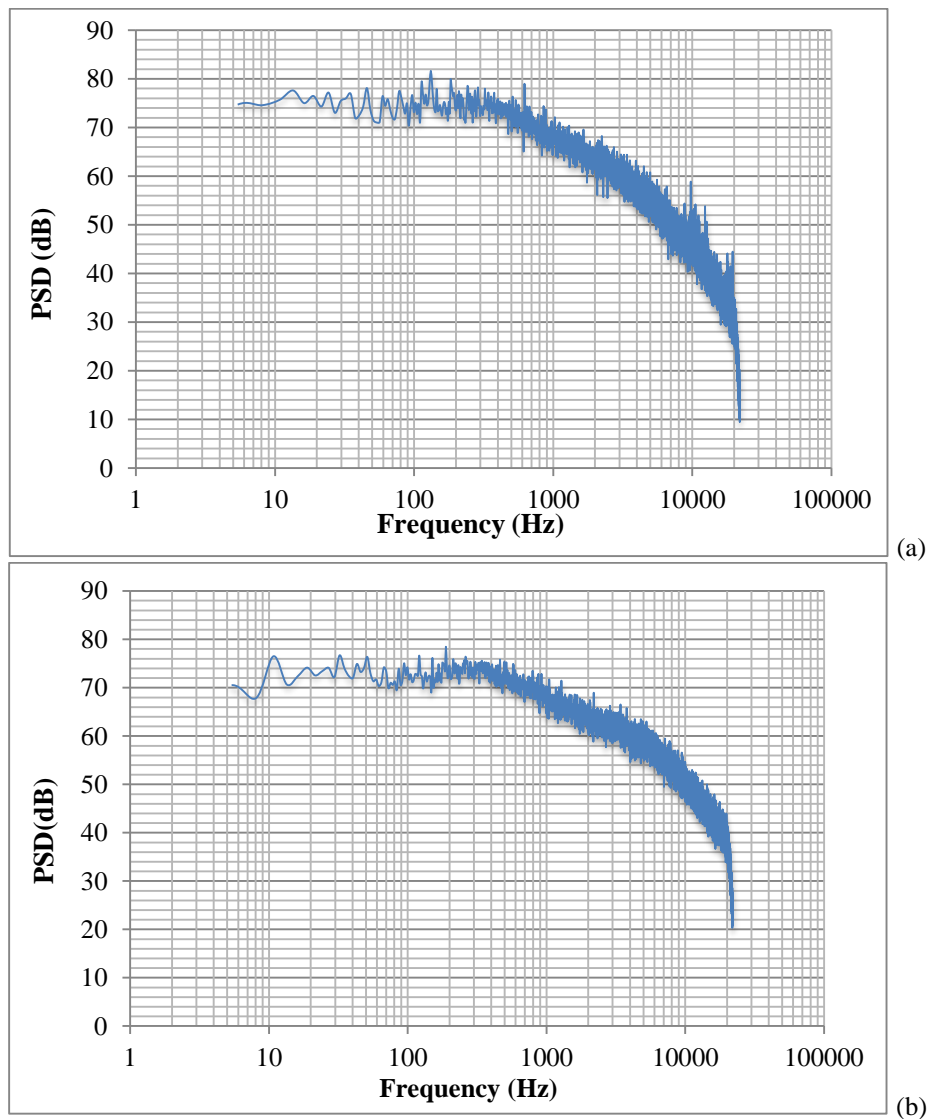
Outdoor Test of Modified Car Side Mirror

A prototype of a mirror that has been simulated by CFD was made by CNC milling. Next, a manufactured mirror was mounted on Tiba instead of the original mirror. As with the original Tiba mirror, the outdoor test was performed at three forward speeds: 80, 100, and 120 km/h. The sound pressure level was measured by a microphone and recorded by a data logger. The configuration of the instrument and the modified car side mirror is exemplified in Figure 16.



Figure 16. Mounted modified car side mirror on Tiba

The results of outdoor tests are shown in Figure 17. As with the original mirror, there is a correlation between CFD simulation and PSD recorded.



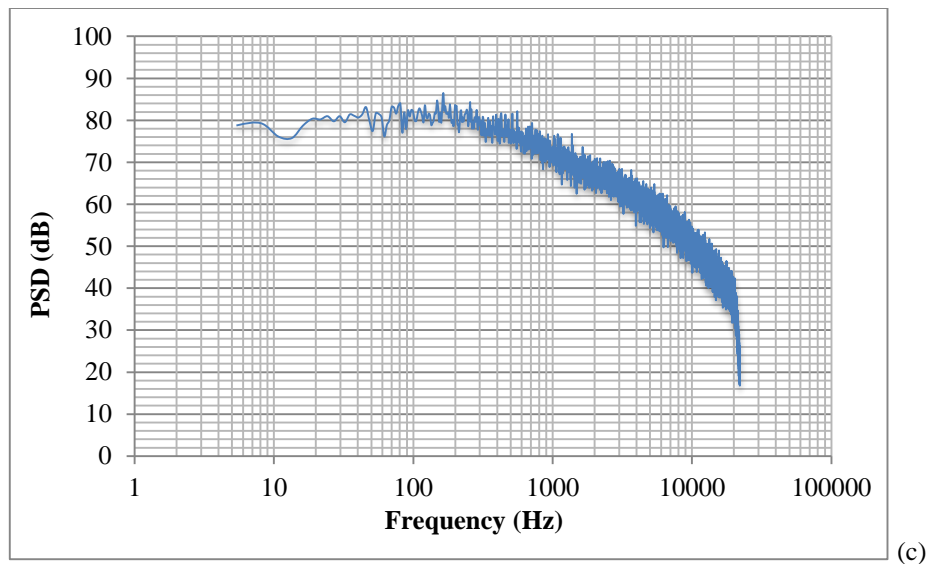


Figure 17. The maximum sound pressure level measured in outdoor test: (a) 80 km/h, (b) 100 km/h, and (c) 120 km/h

The maximum sound pressure levels were acquired at 79, 83, and 88 db at 80, 100, and 120 km/h, respectively. The comparison between the original mirror and the modified mirror in measured sound pressure level is demonstrated in Figure 18. The percent reduction in sound pressure levels ranges between 8.13 and 12.87%. It is reached by correction of side mirror geometry and restriction of the fluctuating pressure area and turbulent flow in this zone.

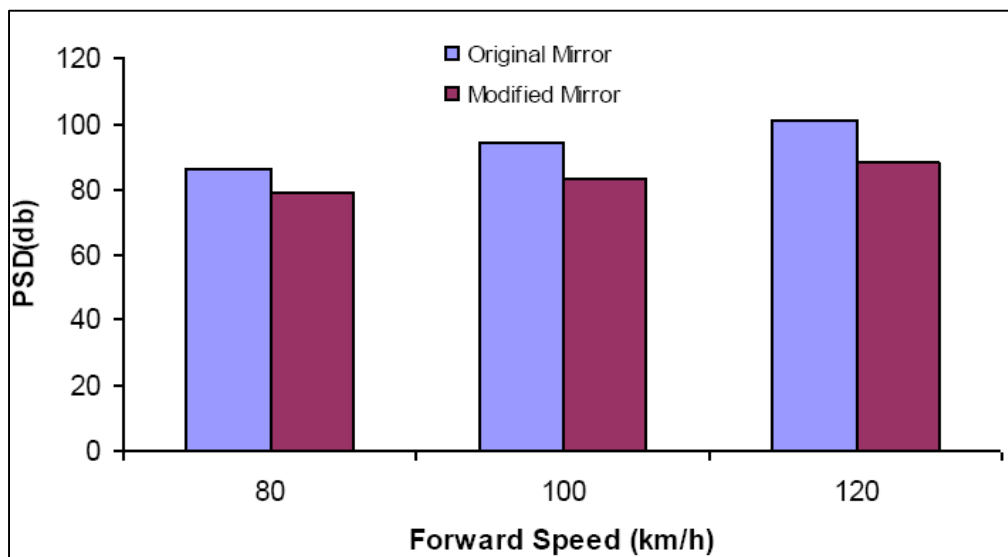


Figure 18. Comparison between original and modified mirror in measured sound pressure level

4. Conclusion

Because some aspects of human life are spent in vehicles on a daily basis, the comfortability of such vehicles is critical. There are many sources of noise and vibration in vehicles that must be modified by engineering studies. One of the noises transmitted to the vehicle's passengers is produced by the car's side view mirror. The current paper's aim is to study airborne noise generated by airflow of the original car side mirror of Tiba and geometry optimization of that with two approaches: CFD modeling and outdoor tests. The pressure sound level of the original Tiba side view mirror was measured and reached between 86 and 101 db. It is normal for the sound level to increase when the forward speed of a vehicle increases. The provided finite element model of the side view mirror shows turbulent airflow contours and negative pressure. Through this CFD simulation, critical points in the fluctuating pressure zone behind the mirror that generate negative pressure and turbulent flow that lead to noise generation were obtained. In a 2D simulation, a cross-section area with a minimum sound pressure level was achieved, and it was extruded into a 3D model. The CFD simulation of the 3D model shows a noise reduction of around 7 to 12%. The velocity contours revealed that the turbulent airflow generated by the side mirror was converted to laminar flow approximately. Also, tests were conducted on a 3D model that was constructed. The results confirmed that noise reduction occurred between 8.13 and 12.87%. To sum up, this novel geometry can be mounted on Tiba to have lower aeroacoustic noise due to mirror aerodynamics.

5. Declarations

5.1. Author Contributions

M.G., R.N. and A.H.A. contributed to the design and implementation of the research, to the analysis of the results and to the writing of the manuscript. All authors have read and agreed to the published version of the manuscript.

5.2. Data Availability Statement

The data presented in this study are available in article.

5.3. Funding

The authors received no financial support for the research, authorship, and/or publication of this article.

5.4. Declaration of Competing Interest

The authors declare that they have no known competing financial interests or personal relationships that could have appeared to influence the work reported in this paper.

6. References

- [1] Watkins, S., & Oswald, G. (1999). The flow field of automobile add-ons - With particular reference to the vibration of external mirrors. *Journal of Wind Engineering and Industrial Aerodynamics*, 83(1–3), 541–554. doi:10.1016/S0167-6105(99)00100-2.
- [2] Batel, M., Marroquin, M., Hald, J., Christensen, J. J., Schumacher, A. P., & Nielsen, T. G. (2003). Noise source location techniques-simple to advanced applications. *Sound and Vibration*, 37(3), 24-38.
- [3] Jaitlee, R., Alam, F., & Watkins, S. (2004). Pressure measurements on an automobile side rear view mirror. In *The 15th Australasian Fluid Mechanics Conference*, 13-17 December 2004, The University of Sydney, Sydney, Australia.
- [4] Jaitlee, R., Alam, F., & Watkins, S. (2005). Vibration of Automobile Side View Mirror Due to Aerodynamic Inputs. *International Conference on Mechanical Engineering, (ICME2005) 28 - 30 December 2005, Dhaka, Bangladesh*.
- [5] Kim, J. H., & Han, Y. O. (2011). Experimental investigation of wake structure around an external rear view mirror of a passenger car. *Journal of Wind Engineering and Industrial Aerodynamics*, 99(12), 1197–1206. doi:10.1016/j.jweia.2011.10.002.
- [6] Plunt, J. (2005). Examples of using transfer path analysis (TPA) together with CAE-models to diagnose and find solutions for NVH problems late in the vehicle development process. In *SAE Technical Papers*. SAE Technical Paper. doi:10.4271/2005-01-2508.
- [7] Vehicle Safety Standard. (2006). Department Of Transport and Regional Services. *Vehicle Standard (Australian Design Rule 14/01 – Rear Vision Mirrors)*, Australia.
- [8] Grahs, T., & Othmer, C. (2006). Evaluation of aerodynamic noise generation: Parameter study of generic side mirror evaluating the aeroacoustic source strength. *Proceedings of the European Conference on Computational Fluid Dynamics (ECCOMAS CFD 2006)*, 1–14.
- [9] Ask, J., & Davidson, L. (2006). The sub-critical flow past a generic side mirror and its impact on sound generation and propagation. *Collection of Technical Papers - 12th AIAA/CEAS Aeroacoustics Conference*, 3, 1925–1944. doi:10.2514/6.2006-2558.
- [10] Bremner, P., Aprilia, V., & Mar, D. (2014). Developing aerodynamic design diagnostics for control of interior wind noise. *Proceedings of the 14ème Congrès Français d'Acoustique*, 22-25.
- [11] Vanco, L., & Pierce, A. D. (1998). *Acoustics: An Introduction to Its Physical Principles and Applications*. *Computer Music Journal*, 22(2), 68. doi:10.2307/3680971.
- [12] Dawi, A. H., & Akkermans, R. A. D. (2019). Direct noise computation of a generic vehicle model using a finite volume method. *Computers and Fluids*, 191, 104243. doi:10.1016/j.compfluid.2019.104243.
- [13] Yao, H. D., & Davidson, L. (2018). Generation of interior cavity noise due to window vibration excited by turbulent flows past a generic side-view mirror. *Physics of Fluids*, 30(3), 36104. doi:10.1063/1.5008611.
- [14] He, Y., Schröder, S., Shi, Z., Blumrich, R., Yang, Z., & Wiedemann, J. (2020). Wind noise source filtering and transmission study through a side glass of DrivAer model. *Applied Acoustics*, 160, 107161. doi:10.1016/j.apacoust.2019.107161.
- [15] Ali, M. S. M., Jalasabri, J., Sood, A. M., Mansor, S., & Shaharuddin, H. (2018). Wind noise from A-pillar and side view mirror of a realistic generic car model, DriAver. *International Journal of Vehicle Noise and Vibration*, 14(1), 38–61. doi:10.1504/IJNV.2018.093109.

- [16] FU, W., & LI, Y. (2021). Noise control of a rearview mirror by using a slotted base support. 3rd International Conference on Industrial Aerodynamics, Changchun, China.
- [17] Pan, Z., Hou, H., Lu, W., Ji, C., Du, M., Yin, X., & Bai, C. (2021). Experimental and numerical investigation on the flow-induced interior noise based on pellicular analysis. *International Journal of Acoustics and Vibrations*, 26(1), 18–27. doi:10.20855/ijav.2020.25.11677.
- [18] Nusser, K., & Becker, S. (2021). Numerical investigation of the fluid structure acoustics interaction on a simplified car model. *Acta Acustica*, 5, 22. doi:10.1051/aacus/2021014.
- [19] Wang, Y. P., Chen, J., Lee, H. C., & Li, K. M. (2012). Accurate simulations of surface pressure fluctuations and flow-induced noise near bluff body at low mach numbers. In *The Seventh International Colloquium on Bluff Body Aerodynamics and Applications*, Shanghai, China, 1334–1348.
- [20] Chu, Y.-J., Shin, Y.-S., & Lee, S.-Y. (2018). Aerodynamic Analysis and Noise-Reducing Design of an Outside Rear View Mirror. *Applied Sciences*, 8(4), 519. doi:10.3390/app8040519
- [21] Wang, Y., Gu, Z., Li, W., & Lin, X. (2010). Evaluation of aerodynamic noise generation by a generic side mirror. *World Academy of Science, Engineering and Technology*, 37, 1288–1295. doi:10.5281/zenodo.1071039.
- [22] Olsson, M. (2011). *Designing and Optimizing Side-View Mirrors*, Chalmers University of Technology, Division of Vehicle Engineering and Autonomous Systems, Master's Thesis, Göteborg, Sweden.
- [23] Georgiev, V. B., Krylov, V. V., & Winward, R. E. T. B. (2006). Simplified modelling of vehicle interior noise: Comparison of analytical, numerical and experimental approaches. *Journal of Low Frequency Noise Vibration and Active Control*, 25(2), 69–92. doi:10.1260/026309206778494300.
- [24] Hu, H. X., Tang, B., & Zhao, Y. (2016). Active control of structures and sound radiation modes and its application in vehicles. *Journal of Low Frequency Noise Vibration and Active Control*, 35(4), 291–302. doi:10.1177/0263092316676400.
- [25] Spannheimer, H., & Freymann, R. (1997). Infrasound and low frequency noise in the passenger compartment of vehicles. *Journal of Low Frequency Noise Vibration and Active Control*, 16(4), 219–227. doi:10.1177/026309239701600401.
- [26] Chu, Y. J., Shin, Y. S., & Lee, S. Y. (2018). Aerodynamic analysis and noise-reducing design of an outside rear view mirror. *Applied Sciences (Switzerland)*, 8(4), 519. doi:10.3390/app8040519.
- [27] Shao, J., Zeng, T., Wu, X., & Wang, C. (2019). Numerical prediction of interior noise due to fluctuation surface pressure with an idealized side mirror. *Inter-Noise 2019 Madrid - 48th International Congress and Exhibition on Noise Control Engineering*, 259(4), 5639–5650.